Characterization of Monoclonal Antibodies Against Quiescin Sulfhydryl Oxidase 1

by

Calvin John Koelbel

A Thesis Presented in Partial Fulfillment
of the Requirements for the Degree
Master of Science

Approved April 2019 by the
Graduate Supervisory Committee:

Douglas Lake, Chair
Qiang "Shawn" Chen
Thai Ho

ARIZONA STATE UNIVERSITY

May 2019

ABSTRACT

Quiescin sulfhydryl oxidase 1 (QSOX1) is an enzyme that catalyzes disulfide bond formation by oxidizing two free sulfhydryl groups. QSOX1 consists of a thioredoxin (Trx) and an ERV (essential for respiration and viability)/ALR (augmenter of liver regeneration) domain which each contain CxxC motifs that work to bind to substrates and shuttle electrons to a flavin adenine dinucleotide (FAD) cofactor that accepts the electrons and reduces molecular oxygen to hydrogen peroxide. Investigation of the role of QSOX1 in cancer progression started when it was found at higher abundance in pancreatic ductal adenocarcinoma (PDA) patient plasma compared to healthy normal donor plasma. Increased expression in QSOX1 has been further identified in breast, lung, kidney, prostate, and other cancers. QSOX1 expression is associated with cell proliferation and invasion *in vitro* and tumor growth *in vivo*. Additionally, the enzymatic activity of QSOX1 in the extracellular matrix (ECM) is important for cell invasion *in vitro*. Small molecule inhibitors of QSOX1 have been shown to have antitumorigenic properties *in vitro* and *in vivo*. It was hypothesized that monoclonal antibodies (mAbs) against QSOX1 would inhibit cell invasion *in vitro*. In this work, mice were immunized with eukaryotic-derived rQSOX1 for generation of hybridomas. Hundreds of hybridoma clones were screened by enzyme-linked immunosorbent assay (ELISA) and a fluorescent QSOX1 activity assay. Multiple rounds of subcloning and screening identified 2F1.14 and 3A10.6 as mAbs of interest. The genes for the variable regions of the antibodies were rescued and sequenced. The sequences were aligned with

the variable region sequences of another published αQSOX1 mAb scFv492.1. 2F1.14 inhibits the enzymatic activity of QSOX1 by binding to the active site of QSOX1, which was determined by epitope mapping against mutants of QSOX1 that contained mutations in the active site. 3A10.6 did not appear to inhibit the function of QSOX1 in the activity assay; however, it, along with 2F1.14, suppressed tumor invasion in a 3D invasion model. These findings support the developing idea that QSOX1 is a viable target for cancer treatment because targeted inhibition of QSOX1 extracellularly reduced invasive activity. The mAbs and rQSOX1 variants produced here can serve as tools in furthering the characterization of QSOX1 and its role in cancer.

DEDICATION

To my eternal companion, Megan Koelbel, who has given me something to look forward to every single day of my life and every day to come.

To Bobby, Cole, Tyler, Dan, and David, whose late nights playing video games, board games, and Magic: the Gathering over the past decade have served as an outlet for me to relax and not stress about everything going on.

To my sister, Courtney, whose guidance and example showed me that I can do everything and anything I want to, no matter what anyone else says.

To my parents, Tom and Lidia, who have loved and supported me unconditionally for my entire life and have taught me the most valuable lesson of all: happiness and family are the only important things in life.

And lastly, to my Grandma Lee, whose perseverance and success through immense adversity has shown me that I can overcome any obstacles, and whose two victories over cancer inspired my desire to pursue cancer research.

ACKNOWLEDGEMENTS

I would like to thank whoever in the School of Life Sciences decided that freshman needed an introductory course on something that I don't even remember anymore.

I thank Douglas Lake, whom I met as a freshman in that introductory course and just so happened to find on an ASU research mentor database at the same time. I will forever be grateful for the opportunity I was given to work in his lab for a summer, based almost entirely on the fact that I thought his research was pretty cool, and for the relationship that has grown from that, spanning 4 years now, and continuing into a Ph.D. program. The scientific thinking skills I developed under his mentorship have contributed significantly to my success in the lab and in other facets of my life, and I will always appreciate his famous (to me) quote after a failed experiment: "This is why it's called REsearch!"

I thank Shawn Chen, whose knowledgeable comments and positive remarks after I send him data, whether it was good news or bad news, helped motivate me to never give up. I thank Thai Ho, who is an inspiration to me professionally and intellectually, and who endured what may have been the most awkward two days of shadowing from an undergraduate ever.

I thank Amber Fifield, Natalie Mitchell, and Paul Hanavan whose drives to discover and learn (and finish their Ph.D.'s) have been an example to me to follow the data, and not take anything at face value, but to seek out truth myself. I thank Kirsten

Pfeffer, Alexa Roeder, and Francisca Grill for being incredible friends in and out of the lab and letting me vent and complain to them when things piled up. Lastly, I thank Yvette Ruiz, a.k.a. the Queen of the Lake Lab, who trained me to be a good lab mate and gave me the foundational knowledge I needed to prosper; and who has graciously forgiven me for breaking many things in the lab.

TABLE OF CONTENTS

Page

Page

LIST OF FIGURES

Figure Page

INTRODUCTION

Cancer is the second leading cause of death in the United States and is on the rise to become the leading cause overall (Centers for Disease Control and Prevention). Men and women are at a 38.4% risk of being diagnosed with cancer during their lifetime. 49.4% of cancer deaths are caused by bladder, breast, renal, lung, pancreatic, and prostate cancers, with pancreatic cancer having an astonishingly low survival rate of 8.5% within five years of diagnosis (National Cancer Institute). Quiescin sulfhydryl oxidase 1 (QSOX1) is associated with each of these tumor types, and the amount of evidence supporting the idea that QSOX1 has significant involvement in cancer progression has been growing over the past decade.

QSOX1 is an enzyme that catalyzes formation and shuffling of disulfide bonds of client proteins in the endoplasmic reticulum (ER), Golgi apparatus, and in the extracellular matrix (ECM) (Hoober et al. 1996; Mairet-Coello et al. 2004; Jaje et al. 2007). It was initially discovered as being a part of a group of genes that are expressed in human lung fibroblasts that had reached quiescence, originally being named Q6 in a group called quiescins, which also includes ECM proteins decorin and collagen (Coppock et al. 1991). There are two forms of QSOX1, a short form (QSOX1-S) and a long form (QSOX1-L). The QSOX1-S is 604 amino acids long, while QSOX1-L is 747 amino acids long. The additional 143 amino acids contained in QSOX1-L is added C-terminal to QSOX1-S and contains a transmembrane domain (Radom et al. 2006). The short form of QSOX1 is dominantly excreted by cells (Stirling et al. 2007), and there is evidence that

shows that QSOX1-L is proteolytically cleaved into QSOX1-S, removing the transmembrane domain, allowing for the secretion of QSOX1-S into the ECM (Rudolf, Pringle, and Bulleid 2013).

In addition to the transmembrane domain, QSOX1 contains three major domains: two Trx-like (thioredoxin) domains (Trx1 and Trx2), an ERV (essential for respiration and viability)/ALR (augmenter of liver regeneration) domain, and a FAD (flavin adenine dinucleotide)-binding domain (Coppock, Cina-Poppe, and Gilleran 1998; Hoober et al. 2002). There are also three CxxC motifs (two cysteines separated by any two amino acids); one located in the Trx1 domain (C70-C73), one in the ERV/ALR domain (C449-452), and one a few amino acids downstream of the FAD-binding domain (C509-512) (Hoober et al. 2002). The mechanism of QSOX1 utilizes two of these CxxC motifs and a

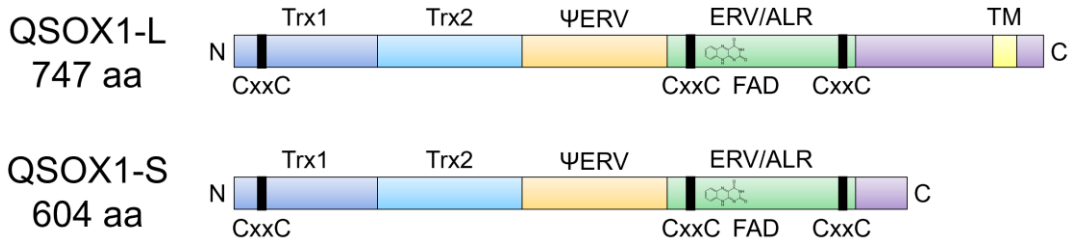

Figure 1: Schematic of the domains and motifs of QSOX1. Trx domains are in blue, pseudo ERV domain is denoted with ΨERV in yellow and ERV/ALR in green. CxxC motifs and FAD cofactor binding are labelled.

FAD molecule to generate disulfide bonds from free sulfhydryl groups in substrates (Heckler et al. 2008). This mechanism was determined by mutating the cysteine residues in the motifs, which found that mutation of C70, C73, C449, and C452 caused almost complete loss of enzymatic function. The C509-C512 CxxC motif has been found to have

no contribution to the enzymatic activity of QSOX1 in a study in which the motif was mutated and enzymatic activity remained (Heckler et al. 2008)

The enzymatic activity of QSOX1 has been characterized utilizing a number of substrates including dithiothreitol (DTT) and reduced RNase A in fluorescence-based assays (Raje, Glynn, and Thorpe 2002), as well as a luciferase from copepod *Gaussia princeps* (GLuc) in a luminescence-based assay (Yu et al. 2018). The activity assays with DTT and reduced RNase A rely on the production of hydrogen peroxide (H_2O_2) as a byproduct of QSOX1 forming disulfide bonds from free sulfhydryl groups. H_2O_2 is consumed in a secondary reaction with horseradish peroxidase (HRP) and homovanillic acid (HVA) in which HRP creates a fluorescent dimer of HVA. The fluorescence of the HVA dimer is proportional to the amount H_2O_2 present in the assay, and thusly is proportional to the activity of QSOX1. The luminescence assay utilizes GLuc, which has the distinct characteristic of containing ten cysteines that are involved in disulfide bonding and has little to no luminescent activity when reduced. QSOX1 oxidizes and folds reduced GLuc, creating a functional luciferase. When GLuc substrate (coelenterazine) is added, a measurable luminescent signal is generated. This assay works independently of any H_2O_2 detection reaction, which is beneficial because interaction of substrates or potential inhibitors with HRP or HVA is no longer a concern. QSOX1 activity can also be measured by Clark-type electrode, which measures the amount of molecular oxygen in a solution using a platinum surface that electrolytically reduces oxygen by donating electrons ran through the platinum electrode and a silver electrode (Clark et al. 1953). When QSOX1 is added, the amount of oxygen reacting with the

platinum electrode decreases as more substrate is consumed (Hoober et al. 1996; Raje and Thorpe 2003). This method provides another way of measuring the activity of QSOX1 independent of a secondary reaction; however, this method does not allow for high-throughput analysis of different conditions for QSOX1 activity.

The current model of the mechanism of QSOX1 is that substrates initially interact with the C70-C73 motif in the Trx-like domain by creating a disulfide bond with C73, after which electrons are shuttled to the C449-C452 motif and are ultimately donated to FAD, where molecular oxygen is reduced to hydrogen peroxide as result of substrate oxidation (Heckler et al. 2008; Alon et al. 2012). The ability of the C70-C73 motif to shuttle electrons to the C449-C452 motif relies on a hinge-like action that brings the two motifs at opposite ends of the enzyme together after a substrate has interacted with the C70-C73 motif (Gat et al. 2014). This hinge-like action has been associated with a cis-proline (P119) which has been shown to be crucial to both the enzymatic and biological activity of QSOX1. Mutation of this proline residue to a threonine resulted in loss of enzymatic function and exogenous addition of this P119T mutant to fibroblast cell culture causes disruption of fibronectin in the ECM (Javitt et al. 2018). QSOX1 has been shown to be involved with other ECM proteins as well, including laminin α4. WI-38 lung fibroblast QSOX1 knockdowns had significantly lesser amounts of laminin deposition into the ECM, which was later characterized to be laminin α4 specifically (Ilani et al. 2013).

Investigation of the role of QSOX1 in cancer started in 2009 when a peptide (NEQEQPLGQWHLS) from the extra 143 amino acids contained in QSOX1-L was

found through mass spectrometry analysis of the plasma peptidome of patients with pancreatic ductal adenocarcinoma (PDA) (Antwi et al. 2009). This peptide was found in 16 out of 23 patients with PDA and was absent from 42 healthy normal donors. This study marked QSOX1 as a potential marker of cancer, and the reason for its expression only in pancreatic cancer patients compared to normal healthy donors was investigated. QSOX1 expression was suppressed by stably transducing two pancreatic cancer cell lines (Panc-1 and BxPC3) with short-hairpin RNAs (shRNAs) targeting QSOX1 and looking at the effect on hallmark cancer characteristics (Katchman et al. 2011). QSOX1 knockdown resulted in several interesting changes: cell proliferation and invasion both decreased in three different knockdown clones. The mechanism in which QSOX1 is involved in invasion was studied, and it was found that QSOX1 knockdowns caused a decrease in matrix metalloproteinase (MMP) activity, specifically MMP-2, by gelatin zymography compared to shScramble controls. Additionally, the transcription levels of MMPs were found to be unaffected by the knockdown of QSOX1, supporting the idea that QSOX1 posttranslationally activates MMPs.

The observations of QSOX1 and its role in pancreatic cancer were then looked at in breast cancer (Katchman et al. 2013). The same shRNA QSOX1 knockdowns were made in MCF7, BT549, and BT474 cell lines. Similar observations were made in these knockdown experiments: cell proliferation and cell invasion decreased compared to shRNA controls. Again, MMPs were investigated; however, in the breast cancer cell lines, it was MMP-9 that showed decreased activation in QSOX1 knockdown cells. This data supported the ongoing hypothesis that QSOX1 was a potential prognostic marker for

aggressive tumors. On the contrary, there was another group that previously published data suggesting that QSOX1is a marker of a good prognosis for patients (Pernodet et al. 2012). The data showed that knockdown of QSOX1 expression caused a decrease in cell proliferation, and a decrease in cell invasion. A third group set out to look at expression of QSOX1 and its prognostic value by immunohistochemistry (IHC) on breast cancer patient tumors (Knutsvik et al. 2016). Tissue staining with αQSOX1 antibodies was given a score on a staining index, and those scores were matched with different histopathological variables. It was determined from this study that QSOX1 expression was associated with markers of poor prognoses, like high grade, hormone receptor negativity, human epidermal growth factor receptor 2 (HER2) positivity, and increased tumor cell proliferation, as well as lower survival rates. These findings support the hypothesis that QSOX1 is a biomarker for more invasive, aggressive tumors. This hypothesis is further supported by data from lung and prostate cancer investigations, in which QSOX1 was associated with high grade, aggressive tumors (Baek et al. 2018; Sung et al. 2018). Collectively, these data suggest that QSOX1 is a viable biomarker and target for treatment.

Ebselen has been identified as a small molecule inhibitor of QSOX1 (Hanavan et al. 2015). Treatment of pancreatic and renal cancer cell lines with ebselen caused significant decreases in cell invasion, similarly to the effect of knocking down QSOX1 expression with shRNAs. Additionally, when nude mice with human tumors were treated with ebselen, tumor growth was suppressed over a 28-day period. The interaction between ebselen and QSOX1 was determined by liquid chromatography mass

spectrometry (LC-MS) to be covalent binding to sulfhydryl groups. Further, it was shown by CDAP (1-Cyano-4-dimethylaminopyridinium tetrafluoroborate) treatment and matrix assisted laser desorption/ionization mass spectrometry (MALDI-MS) that the free cysteines available for ebselen to bind to are C165 and C237. These results suggest that drugs targeting QSOX1 may serve as viable treatment options for slowing the progression of tumors in patients.

With mounting evidence supporting the notion that the enzymatic activity of QSOX1 facilitates cell invasion and tumor growth, the hypothesis that inhibiting QSOX1 would have clinically relevant anti-neoplastic effects continues to grow stronger. In continuation with this idea, it was hypothesized that monoclonal antibodies against QSOX1 could inhibit tumor cell invasion *in vitro*. Additionally, development and characterization of these antibodies could serve as an important tool in future studies of QSOX1; for example, in determining localization, quantifying concentration in fluid samples, etc.

In this work, QSOX1 was cloned and expressed recombinantly in a eukaryotic expression system along with three mutants of QSOX1. Hybridomas were made against rQSOX1 and screened for binding and inhibition of QSOX1 activity. Two monoclonal antibodies were selected, 2F1.14 and 3A10.6. The variable region genes of these two antibodies were cloned and sequenced. The epitope of 2F1.14 was mapped by evaluating binding of the mAbs to rQSOX1 mutants. Lastly, both mAbs were characterized on a cell-free fluorescent QSOX1 activity assay and a 3D invasion assay with patient-derived renal cancer cells.

METHODS

Cell culture

RCJ-41T2 cells were cultured at 37°C with 5% CO_2 in a humidified incubator. HEK293F cells were incubated at 37°C with 8% CO_2 on an orbital shaker set at 135 rpm in a baffled flask. RCJ-41T2 (renal carcinoma) cells were cultured in Dulbecco's Modified Eagle Medium (DMEM) (Corning) supplemented with 10% fetal bovine serum (FBS) (Atlanta Biologicals), 100 µg/mL penicillin/streptomycin (Gibco), and 2 mM GlutaMAX (Gibco). Hybridoma cells were cultured in DMEM supplemented with 5% FBS, 100 µg/mL penicillin/streptomycin, and 2 mM GlutaMAX. HEK293F cells were cultured in Freestyle 293 Expression Medium (Gibco).

rQSOX1 expression and purification

The short form of the QSOX1 gene was amplified from MCF7 cDNA, obtained with a Cells-to-cDNA kit (Ambion), using Phusion Flash Master Mix (Thermo) and cloned into pcDNA3.1 V5/His A (Thermo) using Cold Fusion cloning (System Biosciences). Positive transformants were verified via colony PCR. Verified transformants were cultured in 5 mL LB Amp for 16 hour at 37°C shaking at 225 rpm. Plasmids were extracted from 5 mL cultures in LB-Amp using the GeneJET Plasmid Miniprep Kit (Thermo). Sequences were confirmed by Sanger sequencing (Arizona State University Biodesign Institute Genomics Core). Plasmid was mass-produced in 300 mL cultures and extracted using the Nucleobond Xtra Maxi Plus kit (Macherey-Nagel).

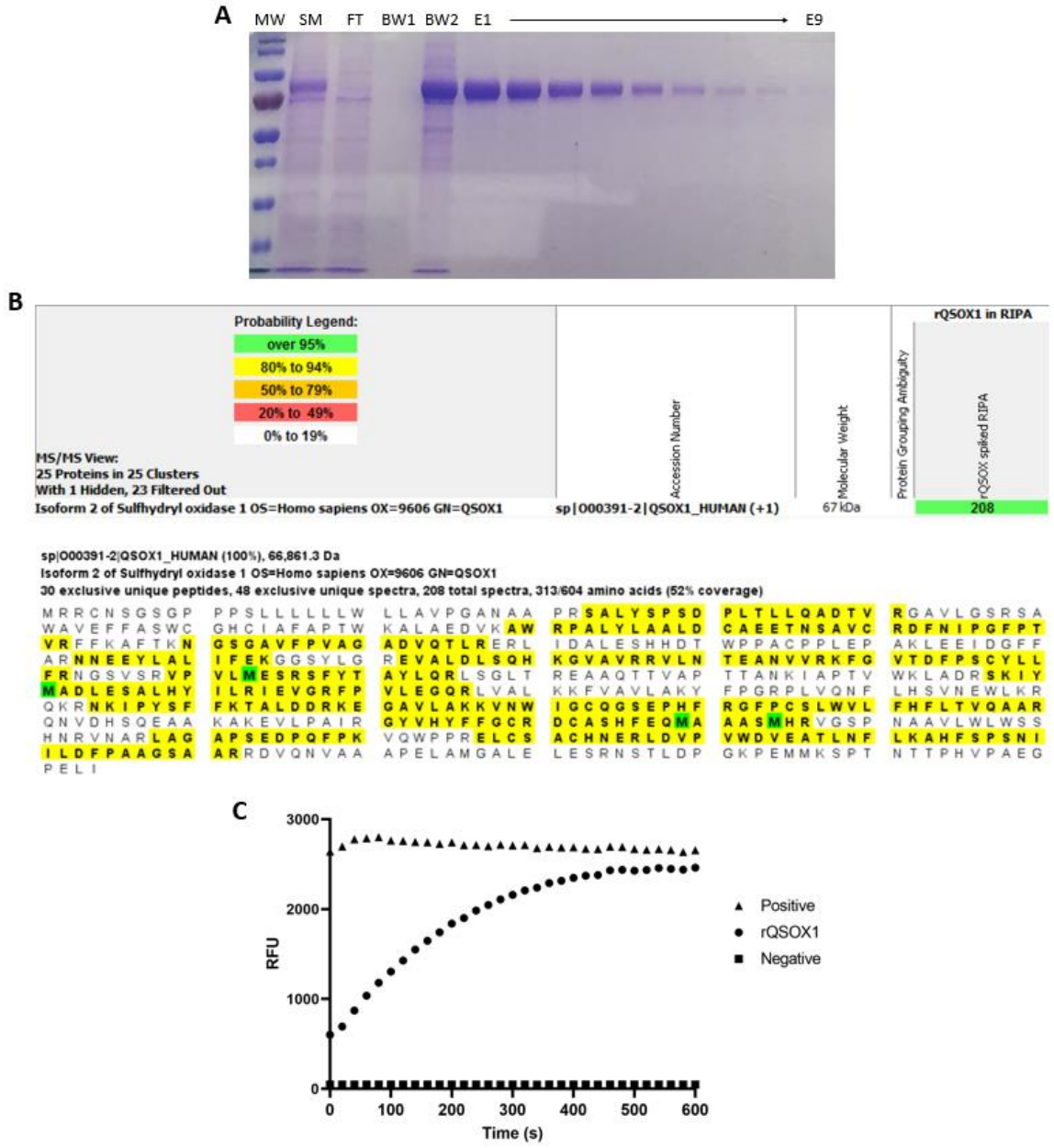

Figure 2: Purification of rQSOX1 produced by 293F cells. A) Elution profile of rQSOX1. MW = 180 kDa PageRuler Prestained Protein Ladder (Thermo), SM = starting material, FT = Ni^{2+}/IDA column flow through, BW = binding buffer wash, E1-8 = elution fractions. **B)** LC-MS data in Scaffold showing rQSOX1 expressed in 293F cells had over 95% probability of being the short form (isoform 2) of QSOX1 with 208 spectral hits and 52% coverage of QSOX1. **C)** Fluorescence-based QSOX1 activity assay of purified rQSOX1 with a positive control (35 µM H_2O_2, no rQSOX1) and a negative control (no rQSOX1). λ_{ex}=320 nm, λ_{em}=420 nm.

293F cells were seeded at $0.7*10^6$ cells/mL 24 hours before transfection for a cell density of $1*10^6$ cells/mL on the day of transfection. An equal ratio of plasmid (µg), Freestyle MAX Reagent (Invitrogen) (µL), and total cell volume (mL) was used (i.e. 30 µg plasmid, 30 µL Freestyle MAX Reagent, 30 mL cell volume). Plasmid and transfection reagent were diluted in OptiPro SFM (Gibco) to a total volume of 0.6 mL each. Plasmid and transfection reagent were combined and incubated together at room temperature for 10 min. The DNA-lipid mixture was added to the 293F cells dropwise while swirling the flask. Transfected cells were incubated at 37°C, 8% CO_2 shaking at 135 rpm for 6-7 days, at which point the media was harvested.

rQSOX1 protein was purified on a Ni^{2+}/IDA His-bind Resin column (EMD Millipore) charged with 100 mM nickel sulfate. The column was washed with 50 mM imidazole to remove any nonspecific proteins that bound. Protein was eluted in fractions of 100 mM imidazole. The column was recharged by removing Ni^{2+} from the column with stripping buffer (20 mM Tris, 100 mM EDTA, 500 mM NaCl), washing with PBS, and storing in 100 mM nickel sulfate. Imidazole elution fractions were run on an SDS-PAGE gel to check for purity (Figure 2). Pure fractions were dialyzed into PBS and concentrated using a 30 kDa Amicon Pro centrifugal filter (EMD Millipore). rQSOX1 was stored at -80°C.

rQSOX1 was run on Orbitrap liquid chromatography mass spectrometry (LC-MS) (Thermo) to confirm the identity of the protein, as previously described (Mitchell et al. 2018). In brief, rQSOX1 was reduced with 10 mM dithiothreitol (DTT) (G Biosciences) for 30 min at 60°C, alkylated with 55 mM iodacetamide (IAA) for 30 min at room

temperature protected from light, and digested with 20 ng/µL trypsin (Thermo) for 16 hours at 37°C at pH=8. 5% formic acid was added to stop trypsin digestion. Samples were lyophilized and rehydrated in 0.01% formic acid, then loaded into autosampler vials.

rQSOX1 mutagenesis

QSOX1 in pcDNA3.1 V5/His A was used as a template for mutagenesis. Primers were designed to introduce missense mutations at t217a, t1345a, and t1354a to change the cysteines in the active site to serines (C73S, C449S, C452S). The point mutation was introduced in the middle of a 24-nucleotide long primer. These primers were used with the normal forward and reverse primers to amplify fragments in the 5' and 3' directions from the mutation site. These fragments were spliced by overlap extension (SOE) to generate the complete mutant QSOX1 gene. Mutant genes were cloned, expressed, purified, and stored as before with the short form of QSOX1.

Generation of monoclonal antibodies

Three Balb/c mice were immunized with 100 µg rQSOX1 in Magic Mouse Adjuvant (Creative Diagnostics) and boosted twice with rQSOX1 two weeks after primary immunization and two weeks after the first boost. The spleen was excised and processed using a 0.44 µM mesh filter (Corning). Splenocytes were fused with P3x63 myeloma fusion partner cells (Kearney et al. 1979) using polyethylene glycol (PEG). Hybridomas were cultured in HAT media for two weeks to kill unfused P3x63 myeloma

cells, while providing nutrients for hybridomas. Unfused B cells died due to their short lifespan in culture. Single-cell cultures of hybridomas were obtained by limiting dilution (1 cell per three wells) and evaluated by enzyme-linked immunosorbent assay (ELISA) against rQSOX1 and chitin synthase 1 (rCTS1) as a control for non-specificity. Clones that produced a high signal by ELISA were subcloned and evaluated by western blot against rQSOX1 and rQSOX1 mutants, and by cell-free fluorescence assay to measure inhibition of QSOX1 activity. The clones 3A10.6 and 2F1.14 were selected for use in further experiments.

ELISA

ELISA was used to screen the hybridoma subclones for binding to rQSOX1. rQSOX1 was coated onto a high-binding, 96-well Costar Assay Plate (Corning) at 1 µg/mL in 100 µL for 1 hour at 37°C. Wells were washed with 200 µL PBST (0.05% Tween-20) twice and blocked with 1% BSA in PBST (Thermo) for 1 hour at room temperature or overnight at 4°C. Wells were probed with 100 µL of hybridoma supernatant for 1 hour at room temperature. Binding of primary antibodies was detected with 100 µL goat anti-mouse (GαM) IgG secondary antibody conjugated with horseradish peroxidase (HRP) (Jackson Immunoresearch Laboratories) diluted at 1:5000 in blocking buffer for 1 hour at room temperature. Wells were developed with 100 µL TMB substrate (BD Biosciences) for 10-15 min. Development was stopped with 100 µL 0.16 M sulfuric acid. Plates were read on a VersaMax tunable plate reader (Molecular Devices).

Western Blot

Western blot screening of αQSOX1 hybridomas involved running 1 μg of rQSOX1 on a SDS-PAGE gel and transferring the proteins to a PVDF membrane. The membrane was blocked with 1% BSA in TBST (Thermo) and cut into strips. Each strip was probed with 1 mL of supernatant from a different hybridoma clone for 1 hour at room temperature. Binding of antibodies from hybridoma supernatants was detected with goat anti-mouse IgG antibody conjugated to alkaline phosphatase (Jackson Immunoresearch Laboratories) diluted 1:5000 in blocking buffer for 1 hour at room temperature. Blots were developed with 1-Step NBT/BCIP (Thermo) for 10-15 min. Development was stopped by washing out developing solution with dH_2O.

Purification of monoclonal antibodies

Media from hybridoma cultures were collected every 5-7 days by centrifuging cells and harvesting the supernatant from the pellet. Supernatant was diluted 1:1 in PBS to neutralize the pH for purification on Protein A/G. Diluted supernatant was run through a column made with 1 mL of Protein A/G Agarose slurry (Pierce). The column was washed twice with PBS, then eluted with 100 mM glycine, pH=3.0. Elution fractions were neutralized with 100 μL 1M Tris, pH=9.0 per 1 mL elution buffer. Supernatant, flow through, and elution fractions were run on an SDS-PAGE gel to analyze purity (Figure 3). Elution fractions with pure antibody were pooled and dialyzed into PBS using a 10 kDa Amicon Pro centrifugal filter. Antibodies were stored at -20°C.

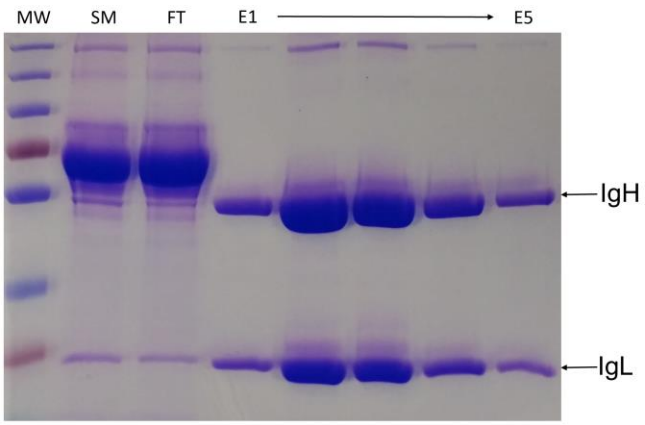

Figure 3: Purification of αQSOX1 mAbs produced by hybridoma clones 2F1.14 and 3A10.6. Elution profile of αQSOX1 mAbs. MW = 180 kDa PageRuler Prestained Protein Ladder (Thermo), SM = starting material, FT = Protein A/G Plus purification flow through, E1-5 = 100 mM glycine elution fractions. Heavy chain (IgH) and light chain (IgL) are labelled at ~50 kDa and ~25 kDa, respectively.

Gene rescue of QSOX1 mAb variable regions

The heavy and light chain variable region genes of 2F1.14 and 3A10.6 were amplified from their respective hybridoma cell cDNA, obtained with a Cells-to-cDNA kit, using published universal degenerate primers for amplification of murine IgG variable heavy and light chain genes (Wang et al. 2000). These primers were altered to add homologous ends to the amplicons which are required for Cold Fusion cloning into pcDNA3.1 V5/His A. The variable regions were cloned and sequenced as before with the short form of QSOX1. The sequences were analyzed in IgBLAST to annotate the framework (FRs) and complementarity determining regions (CDRs). The variable light chain sequences were checked against the sequence of the NS-1 (P3/NS1/1-Ag4-1) myeloma variable light chain sequence (Ning et al. 2012) to verify the determined sequence corresponded to the αQSOX1 mAb. Sequences were aligned with the Fass

group's αQSOX1 single-chain variable fragment mAb 492.1 (Grossman et al. 2013) using EMBOSS Water (EMBL-EBI) on default settings.

Epitope Mapping

MAbs 2F1.14 and 3A10.6 were investigated for binding characteristics to wild type (WT) and mutant QSOX1. 1 µg of WT, C73S, C449S, and C452S QSOX1 was loaded on a SDS-PAGE gel. The proteins were transferred onto a PVDF membrane and blocked with 1% BSA in TBST (Thermo). The blots were probed with 3A10.6 and 2F1.14 at 1 µg/mL in blocking buffer for 1 hour at room temperature with a control lacking primary antibody. Binding of primary antibodies was detected and developed as discussed before, with the exception of the time of development being 5 min.

QSOX1 enzymatic activity assay

The enzymatic activity of rQSOX1 was measured in an assay that utilizes the H_2O_2 byproduct of QSOX1 in a secondary reaction involving the dimerization of homovanillic acid (HVA) by HRP, which produces a fluorescent signal (Raje, Glynn, and Thorpe 2002). This assay was performed in a black opaque 96-well flat-bottom plate (Corning), in which 150 µM DTT (300 µM thiols) was added to 100 nM rQSOX1, 1 mM HVA, 1.4 µM HRP, and 300 µM EDTA in PBS. A positive control consisted of replacing rQSOX1 with 35 µM H_2O_2 to ensure the secondary reaction was functional. H_2O_2 was added with DTT, as HRP immediately acts on H_2O_2 upon its addition. A negative control consisted of all reagents in the assay except rQSOX1. Antibodies were added ~10

minutes before the addition of DTT. The vehicle control was 50% glycerol in PBS. Controls for antibody interaction with the secondary reaction involved adding antibody to the positive control reaction. The final reaction volume was 150 µL. Relative fluorescence was measured in a SpectraMax M Series Microplate Reader (Molecular Devices) at λ_{ex}=320 nm and λ_{em}=420 nm every 20 sec for 10 min at room temperature.

3D invasion assay

A 3D model for invasion experiments reflects a more biologically relevant environment of a tumor growing in tissue (Vinci, Box, and Eccles 2015). RCJ-41T2 cells were seeded in a Costar 96-well Ultra-Low Adhesion U-bottom plate (Corning) at 1,250 cells/mL, or the number of cells that formed a spheroid between 300-500 µm, in 200 µL. Cells were incubated for 4 days at 37°C, 5% CO_2 to form spheroids. Being careful not to disturb the spheroids, 150 µL of media was removed from each well. Antibodies and vehicle treatments were added at a 6X concentration in 50 µL such that the final concentration was appropriate. 100 µL of Matrigel (Corning) was added to each well and incubated for 1 hour at 37°C to allow the matrix to solidify. 100 µL of media was added on top of the solid matrix. The spheroids were incubated in matrix for 7 days, taking bright field images each day. Images were analyzed in ImageJ using grayscale threshold analysis to calculate the size of each spheroid and invading cells.

Loss of enzymatic activity of rQSOX1 mutants

Sanger sequencing results showed that only the intended missense mutations (C73S. C449S, C452S) occurred during mutagenesis of rQSOX1. rQSOX1 active site mutants were added at equal concentration to WT rQSOX1. Reactions were all run for 10 min after addition of DTT substrate. All three mutants showed a loss of enzymatic activity compared to the WT rQSOX1 as indicated by the significantly reduced relative fluorescence in the mutant wells (Figure 3). These results corroborate the results of other groups which also showed that the mutation of cysteines in the CxxC motifs in the active site of QSOX1 causes a loss of function.

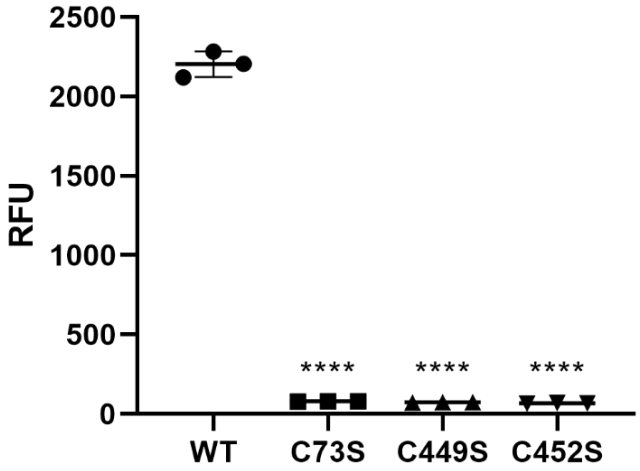

Figure 4: Loss of enzymatic activity by rQSOX1 active site mutants compared to wild-type (WT) rQSOX1. rQSOX1 mutants were added to the QSOX1 enzymatic activity assay at an equal concentration to WT rQSOX1. Relative fluorescence (RFU) was measured 10 min after the addition of DTT. λex=320 nm, λem=420 nm. Error bars are standard deviation. Statistical significance determined by t-test; **** $p<0.0001$.

QSOX1 monoclonal antibody screening

Clones that were positive by indirect ELISA were tested by western blotting. rQSOX1 was probed with supernatant from each hybridoma clone (Figure 4A). 3A10 appeared to be the clone that produced the strongest band while maintaining a low background relative to other high binding antibodies. 2F1 appeared to bind weakly to rQSOX1; however, it bound better than other inhibitory antibodies, which appeared to also bind weakly. Clones that showed moderate to strong binding by western blot were tested in a cell-free fluorescence assay to measure the inhibition of the enzymatic activity of QSOX1. Supernatant from each clone was added to QSOX1 ~10 min before the addition of DTT. 2F1, 1B9, and 1C5 appeared to inhibit QSOX1 (Figure 4B). Because of their characteristics shown in the screening results, 2F1 and 3A10 were chosen subcloned to select for the high-producing clones, resulting in 2F1.14 and 3A10.6

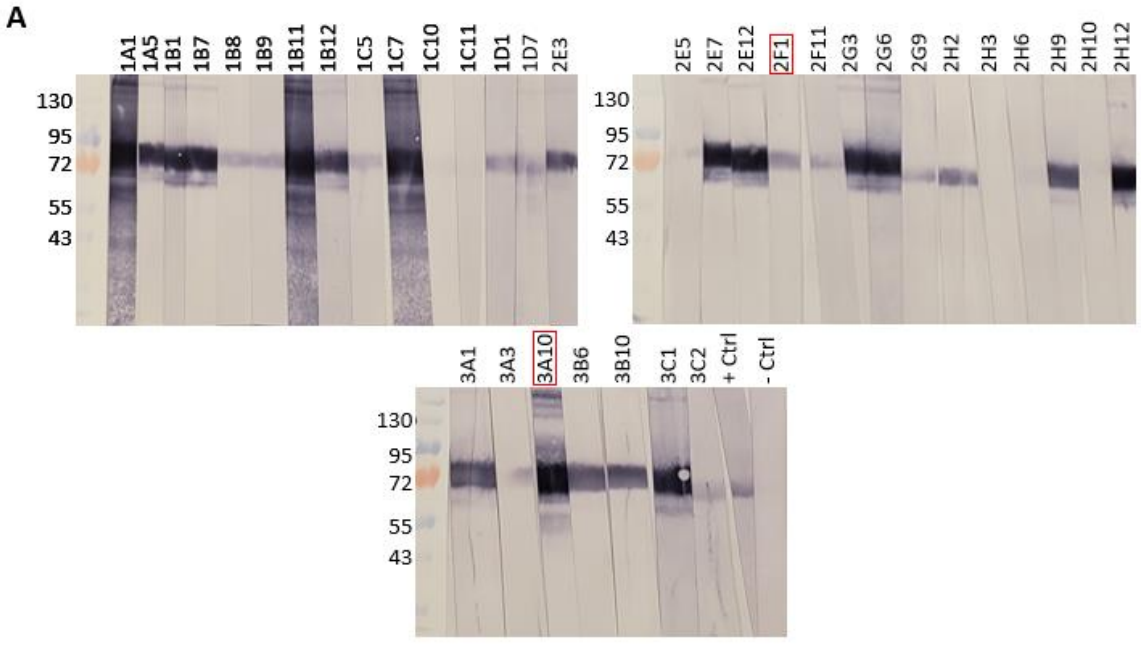

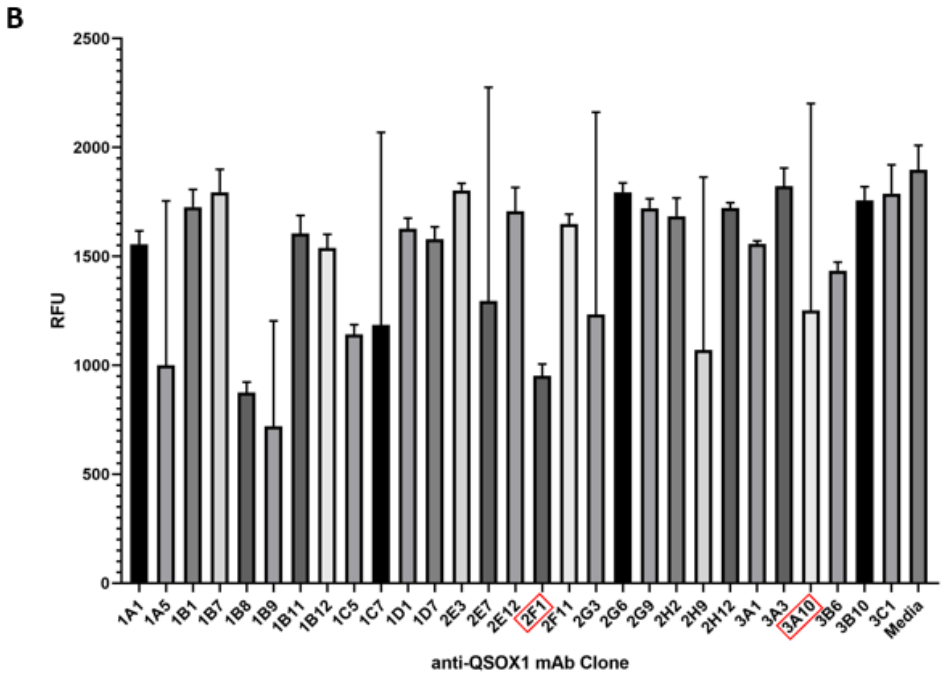

Figure 5: Screening of αQSOX1 hybridomas. A) Western blots showing binding of mAbs in hybridoma supernatant to rQSOX1. Binding of mAbs was detected by GαM IgG-AP and developed with NBT/BCIP. 2F1 and 3A10 are marked in red. **B)** QSOX1 enzymatic activity assay showing inhibition of rQSOX1 by four mAb clones. Hybridoma supernatants were incubated with rQSOX1 for ~10 min before addition of DTT. Relative fluorescence (RFU) was measured 10 min after the addition of DTT. λ_{ex}=320 nm, λ_{em}=420 nm. Error bars are standard deviation. 2F1 and 3A10 are marked in red.

Variable region sequence alignment

The variable heavy and variable light chain genes for both αQSOX1 mAbs were aligned with the Fass group's scFv 492.1 mAb in EMBOSS Water. The 2F1.14 variable heavy gene was 87.3% similar with a gap in CDR3. CDR1 and CDR2 were almost identical with only one amino acid difference in both, with minor similarity (Figure 6A). CDR3, however, was different with only 4 complementary amino acids and a gap in the 2F1.14 sequence. The 2F1.14 variable light gene was almost identical with 94.4%

identity and 98.1% similarity (Figure 6B). Between the three variable light CDRs, all but one residue were identical, and that one residue had minor similarity.

A

```
# Length: 118
# Identity:      92/118 (78.0%)
# Similarity:   103/118 (87.3%)
# Gaps:           1/118 ( 0.8%)
# Score: 487.0
#
#
#=======================================

2F1.14_VH          1 EVQLEESGPGLVAPSQSLSITCTVSGFSLTDYGVTWIRQPPGKGLEWLGV     50
                     :|||::|||||||||||||||||||||||.|||.|:||.|||||||||:
scFv492.1_VH       1 QVQLKQSGPGLVAPSQSLSITCTVSGFSLTGYGVNWVRQSPGKGLEWLGM     50

2F1.14_VH         51 IWGDGSTYYNSALKSRLSISKDDSKSQVFLKMNSLQTDDTAMYYCAGALY    100
                     |||||.|.|.|||||||||:||:||||||||||||||.|:||...|
scFv492.1_VH      51 IWGDGRTDYKSALKSRLSITKDNSKSQVFLKMNSLQTDDTARYFCASDYY    100

2F1.14_VH        101 -DGYYGYWGQGTTLTVSS    117
                      .|.:.||||||.:|||:
scFv492.1_VH     101 GSGSFAYWGQGTLVTVSA    118
```

B

```
# Length: 107
# Identity:     101/107 (94.4%)
# Similarity:   105/107 (98.1%)
# Gaps:           0/107 ( 0.0%)
# Score: 531.0
#
#
#=======================================

2F1.14_VL          1 DIVLTQTHKFMSTSVGDRVSITCKASQDVSTAVAWYQQKPGQSPKLLIYS     50
                     |:|:|||||||||||||||||||||||||||||||||.||||||||:|
scFv492.1_VL       1 DVVMTQTHKFMSTSVGDRVSITCKASQDVSTAVAWYQQKSGQSPKLLIHS     50

2F1.14_VL         51 ASYRYSGVPDRFTGSGSGTDFTFTISSVQAEDLAVYYCQQHYSTPLTFGA    100
                     |||||:|||||||||||||||||||||||||||||||||.||||||
scFv492.1_VL      51 ASYRYTGVPDRFTGSGSGTDFTFTISSVQAEDLAVYYCQQHYSIPLTFGA    100

2F1.14_VL        101 GTKLELK    107
                     |||||||
scFv492.1_VL     101 GTKLELK    107
```

C

```
# Length: 121
# Identity:      60/121 (49.6%)
# Similarity:    82/121 (67.8%)
# Gaps:           6/121 ( 5.0%)
# Score: 298.5
#
#
#=======================================

3A10.6_VH          1 EVQLQQSGGGLVQPGGSMKLSCAASGLTFSDAWMDWVRQSPEKGLEWVAE     50
                     :|||:|||.|||.|..|:.::|..||.:.:...::||||||.|||||:..
scFv492.1_VH       1 QVQLKQSGPGLVAPSQSLSITCTVSGFSLTGYGVNWVRQSPGKGLEWLGM     50

3A10.6_VH         51 IRSKAHNHATYYAESVKGRFTISRDDSKSSVYLQMNSLRAEDTGIYYCTR    100
                     |.....   |.|..::|.|.:|::|:|||.|:|:||||:.:||..|:|..
scFv492.1_VH      51 IWGDGR---TDYKSALKSRLSITKDNSKSQVFLKMNSLQTDDTARYFCAS     97

3A10.6_VH        101 --YGN-PFVYWGQGTLVTVSA    118
                       ||: .|.||||||||||||
scFv492.1_VH      98 DYYGSGSFAYWGQGTLVTVSA    118
```

D

```
# Length: 113
# Identity:      73/113 (64.6%)
# Similarity:    90/113 (79.6%)
# Gaps:           6/113 ( 5.3%)
# Score: 377.5
#
#
#=======================================

3A10.6_VL          1 DIVMTQSPSSLAVSVGEKVTMSCKSSPSLLYSSNQKNYLAWYQQKPGQSP     50
                     |:||||:...::.|||::|:::||:|..:      ...:||||||.||||
scFv492.1_VL       1 DVVMTQTHKFMSTSVGDRVSITCKASQDV------STAVAWYQQKSGQSP     44

3A10.6_VL         51 KLLIYWASTRESGVPDRFTGSGSGTDFTLTISSVKAEDLAVYYCQQYYSY    100
                     ||||:.||.|.:||||||||||||||.|||||:||||||||||:||.
scFv492.1_VL      45 KLLIHSASYRYTGVPDRFTGSGSGTDFTFTISSVQAEDLAVYYCQQHYSI     94

3A10.6_VL        101 PWTFGGGTKLEIK    113
                     |.|||.|||||:|
scFv492.1_VL      95 PLTFGAGTKLELK    107
```

Figure 6: EMBOSS Water alignment of αQSOX1 mAb and Fass group αQSOX1 scFv mAb 492.1 variable region genes. A) 2F1.14 VH, **B)** 2F1.14 VL, **C)** 3A10.6 VH, **D)** 3A10.6 VL. Alignments were run on default settings. Complementarity determining regions (CDRs) are underlined. Identity, similarity, gaps, and score are shown.

The 3A10.6 variable heavy and light chain genes had lesser similarity with 67.8% similarity between the heavy chains and 79.6% similarity between the light chains (Figure 6C and 6D). Additionally, both heavy and light variable regions had six gaps in the CDRs.

Inhibition of rQSOX1 enzymatic activity

2F1.14 and 3A10.6 mAbs were added at 15 µg/mL, 7.5 µg/mL, and 3.75 µg/mL with a vehicle of an equal volume of 50% glycerol in PBS. Additionally, each antibody was added at 15 µg/mL with a vehicle to control wells testing antibody inhibition of the HRP reaction by replacing rQSOX1 with exogenous H_2O_2. This control was included to ensure that any change in fluorescence was the result of the antibodies interacting with rQSOX1 and not with HRP.

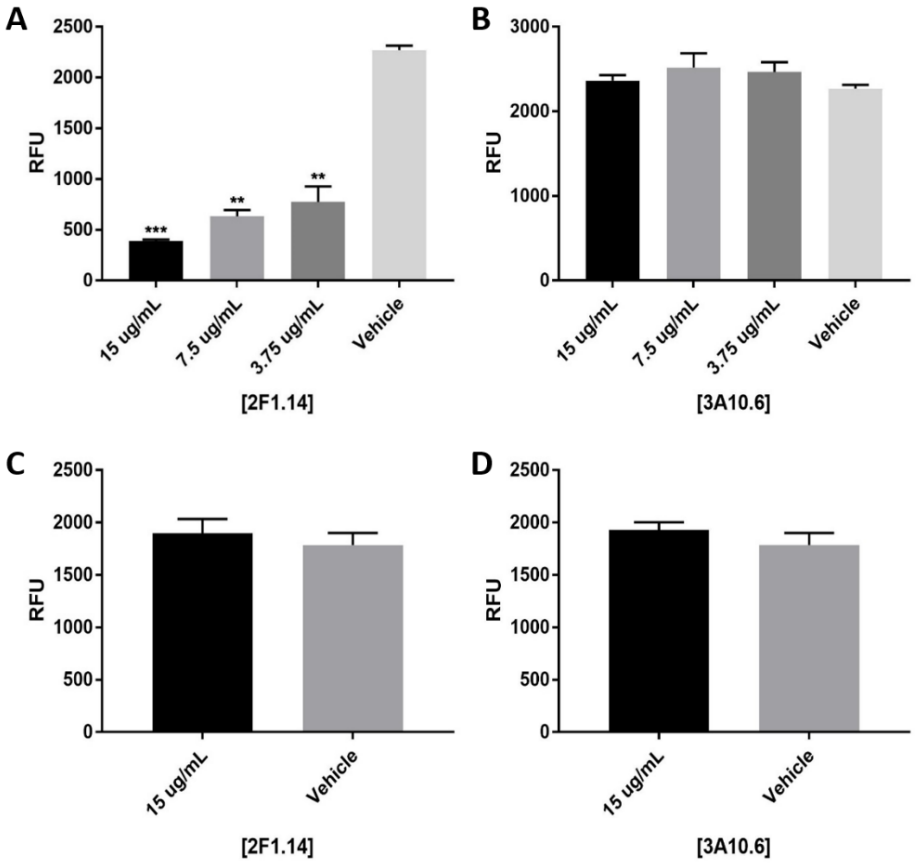

Figure 7: Inhibition of rQSOX1 enzymatic activity by A) 2F1.14 and lack thereof by B) 3A10.6. Anti-QSOX1 mAbs were incubated with rQSOX1 in the presence of HVA and HRP for 10 minutes. DTT substrate was added and the reaction proceeded for 15 minutes at which relative fluorescence was measured. Vehicle is 50% Glycerol in PBS instead of mAb (1.67% Glycerol total). Relative fluorescence units (RFU) are shown on the Y-axis and mAb concentration is shown on the X-axis. Incubation of mAbs with HRP and H_2O_2 in the absence of rQSOX1 to control for potential non-specificity of mAbs binding to and inhibiting HRP is shown for **C)** 2F1.14 and **D)** 3A10.6. Relative fluorescence (RFU) was measured 10 min after the addition of DTT. λex=320 nm, λem=420 nm. Error bars are standard deviation. Statistical significance determined by t-test; *** $p<0.001$, ** $p<0.01$.

The addition of 2F1.14 to the assay caused a significant reduction in fluorescence with increasing concentrations of antibody from ~2200 RFU to <~800 RFU (Figure 7A). In the control wells, 2F1.14 did not cause any significant change in fluorescence with

consistent levels at ~1800 RFU (Figure 7C). On the other hand, addition of 3A10.6 did not cause any significant change in the wells either with rQSOX1 or the control wells without rQSOX1 (Figure 7B and 7D).

This data suggests that 2F1.14 inhibited the activity of rQSOX1. It was possible that 2F1.14 bound to rQSOX1 at or around the active site, blocking the access of substrates for QSOX1. It appeared that 3A10.6 did not inhibit QSOX1, despite showing high signal by ELISA, suggesting that 3A10.6 did not bind in a region critical to the enzymatic function of QSOX1. An important note is that DTT is not a biologically relevant substrate because it is a chemical, not a protein. A more informative experiment would use the reduced form of a known substrate of QSOX1, if they were known. It is likely that laminin α4 and fibronectin are substrates based on data suggesting that QSOX1 plays a role in depositing laminin α4 and fibronectin into the extracellular membrane and could be used in this assay for more biologically relevant results.

Epitope mapping

Mutants of QSOX1 were constructed in which cysteines in the enzymatically active CxxC motifs were mutated to serines (C73S, C449S, and C452S). These mutants were used in western blot analysis of 2F1.14 and 3A10.6 (Figure 8). The western blot shows that while 2F1.14 binds to WT rQSOX1, it does not bind to the C73S mutant of QSOX1. This data suggests that C73 is included in or influences the epitope of 2F1.14. This result corroborates the findings in the QSOX1 enzymatic assay which showed that 2F1.14 inhibited QSOX1 activity likely because C73 in the Trx-like domain is involved

in initial shuffling of sulfhydryls as client proteins are oxidized by QSOX1. Binding of 2F1.14 to the active site of QSOX1 would prevent substrates from accessing the active site, preventing catalysis and oxidation of the substrates.

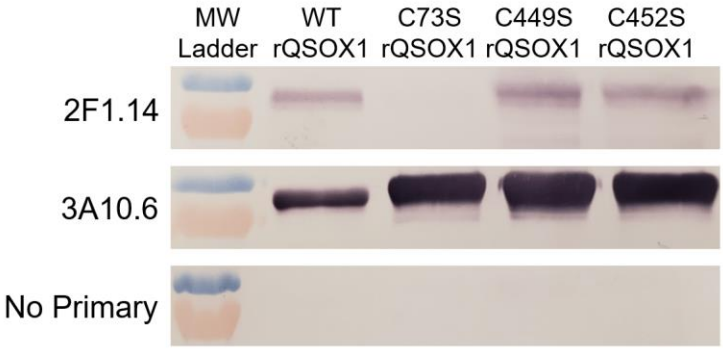

Figure 8: Epitope mapping of 2F1.14 mAb. Wild-type (WT) and mutated QSOX1 were probed with anti-QSOX1 mAbs by western blot. When probed with 2F1.14, bands corresponding to QSOX1 (~72 kDa) appear for all QSOX1 variants except for the C73S QSOX1 mutant. With 3A10.6, bands appear at 72 kDa for each QSOX1 variant.

Inhibition of invasive phenotype in 3D invasion assay

RCJ-41T2 spheroids were treated with 50 µg/mL, 25 µg/mL, 12.5 µg/mL, 6.25 µg/mL, 3.125 µg/mL, and 1.5625 µg/mL of anti-QSOX1 mAb, and Matrigel was prepared according to manufacturer instructions. At 50 µg/mL and 25 µg/mL, both 3A10.6 and 2F1.14 showed significant inhibition of invasion (Figure 9). The observed inhibitory activity of 3A10.6 is curious considering the cell-free enzymatic assay showed that 3A10.6 does not inhibit rQSOX1. One possible explanation for this phenomenon is that 3A10.6 sterically inhibits the biological substrates of QSOX1 from interacting with the active site without binding directly to the active site. As mentioned earlier, the substrate used in the fluorescence assay was DTT, which is a very small molecule and

may be small enough to still interact with QSOX1 at the active site with 3A10.6 bound, while biological substrates may be significantly larger and be blocked by 3A10.6 from interacting with QSOX1.

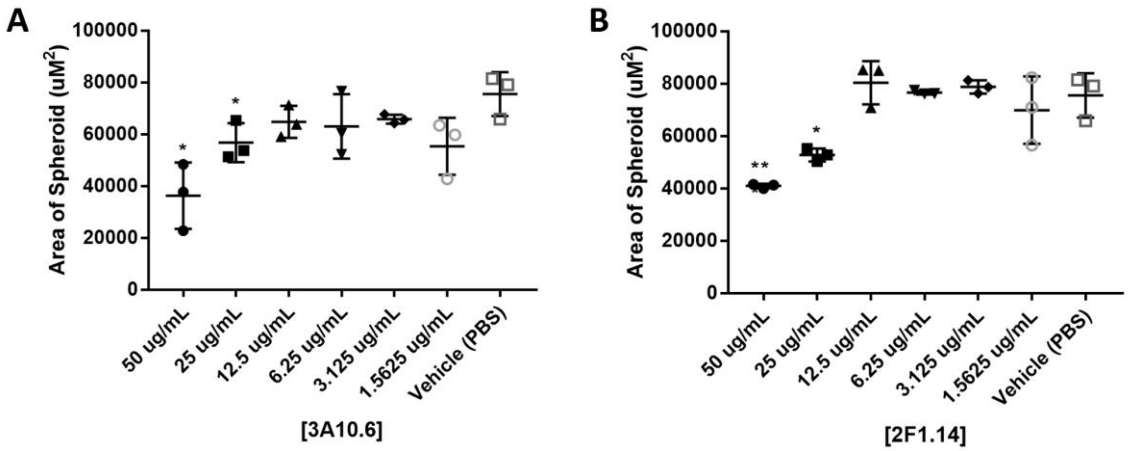

Figure 9: Inhibition of invasion in 3D spheroid invasion assay with RCJ-41T2 cells treated with A) 2F1.14 and B) 3A10.6. Anti-QSOX1 mAbs were incubated with tumor spheroids for 1 h. Matrigel was added and spheroids were incubated for 7 days. Vehicle is PBS instead of mAb. Statistical significance determined by t-test; ** $p<0.01$, * $p<0.05$.

One explanation for the high concentration of mAbs required for suppression of spheroid invasion may be the presence of QSOX1 in Matrigel because Matrigel is made up of the extracellular matrix proteins from mouse sarcoma cells and QSOX1 is secreted into the extracellular matrix. QSOX1 in Matrigel could inhibit the antibody from binding to the spheroid-derived QSOX1, which would presumably reduce the inhibition of cell invasion by the antibodies. However, we have not tested Matrigel for the presence of QSOX1.

Additionally, a rescue experiment is planned to determine if addition of exogenous rQSOX1 will rescue the invasive phenotype of spheroids. This assay would

also include a non-specific mAb to control for the addition of a mAb to the spheroids. When this experiment was conducted, it was presumed that 3A10.6 was the control mAb based on the results of the enzymatic activity assay and the epitope mapping; however, the results of the 3D invasion assay indicate that this presumption is incorrect.

DISCUSSION

Through hybridoma technology, hundreds of clones of αQSOX1 mAbs were generated. After subsequent rounds of screening by ELISA and subcloning by limiting dilution, two mAbs were selected, 2F1.14 and 3A10.6. Compared to 3A10.6, 2F1.14 reacted much less strongly to rQSOX1 based on optical density in ELISA and reactivity to rQSOX1 in western blotting. One might presume the weaker binding is due to lower affinity, but 2F1.14 binds to an epitope containing the active site of the enzyme. It is possible that consistent hinge-like movement of QSOX1 disallows the antibody from binding strongly, or that the state of QSOX1 in which the two distant CxxC motifs are close disallows binding of 2F1.14. Future studies may involve measuring the affinities of both 3A10.6 and 2F1.14 for QSOX1.

The epitope of 2F1.14 was mapped to include or be influenced by C73, as suggested by the absence of a band corresponding to the C73S rQSOX1 mutant by western blot (Figure 6). The alignment of these antibodies with the only other published αQSOX1 mAb sequence suggests that each of these antibodies are novel antibodies. It is interesting to note that scFv 492.1 was also reported to bind to the active site of QSOX1, which is a possible explanation for why the variable region on the light chain of each antibody are so similar (98.1%); however, there is evidence that suggests that it is the heavy chain of the antibody that determines the epitope of the antibody (Wu and Kabat 1970).

Based on the results of the activity assay, it was thought that only 2F1.14 bound and inhibited the activity of QSOX1 while 3A10.6 bound but did not inhibit the activity of QSOX1 because the addition of 2F1.14 caused the fluorescent signal to decrease while the addition of 3A10.6 did not cause any significant change in fluorescent signal. This thought was rejected, however, by the results of the 3D invasion assay which showed that both 2F1.14 and 3A10.6 caused a suppression of invasion by the RCJ-41T2 spheroids, which is likely to be the result of inhibition of QSOX1. As mentioned previously, the substrate used in the enzymatic activity assay was DTT, which is a small, 154 Da molecule. This is important to note because the client substrates of QSOX1 in the ECM that QSOX1 acts on in the 3D invasion assay are unlikely to be as small as DTT. Thus, it is possible that 3A10.6 binds to QSOX1 near but not at the active site, and the presence of the antibody sterically inhibits large, client substrates from accessing the active site of QSOX1. In other words, 3A10.6 does not inhibit the activity of QSOX1; rather, 3A10.6 may inhibit the substrates from entering the active site of QSOX1. This could be further investigated by reducing possible client substrates and testing them in the enzymatic activity assay with the addition of 3A10.6. Possible substrates include ECM proteins like fibronectin, laminin α4, collagen, decorin, and tenascin.

Because of this apparent inhibition of the biological function of QSOX1 by 3A10.6, the 3D invasion assay does not have a proper control for the addition of IgG to the spheroids because 3A10.6 was thought to be that control. To determine if the change in phenotype caused by the addition of 2F1.14 and 3A10.6 was truly due to their interaction with QSOX1, a non-specific mAb would need to be added to the assay. This

antibody should not bind to anything in the assay, so a mAb against a completely unrelated protein could be used. Additionally, rescue of invasive activity with the exogenous addition of rQSOX1 would assist in further determination that the suppression of invasion is caused by the mAb interaction with QSOX1. Additionally, a false rescue with the enzymatically inactive rQSOX1 mutants would control for the addition of QSOX1 causing an increase in invasion, as opposed to the activity of QSOX1 itself.

The inhibitory activity of 2F1.14 and 3A10.6 outside of the spheroids suggests that QSOX1 is secreted by cells and that the activity of QSOX1 that contributes to cell invasion is done in the ECM, not in the Golgi apparatus or ER. This is interesting because one of the foundational studies of QSOX1 in cancer found a peptide from QSOX1-L in PDA patient plasma (Antwi et al. 2009), but QSOX1-L is primarily localized to the Golgi apparatus (Stirling et al. 2007). These observations may support the hypothesis that QSOX1-L is proteolytically processed upon secretion (Rudolf, Pringle, and Bulleid 2013), and that the QSOX1 peptide found in PDA patients was linked to the cleaved portion of QSOX1-L, not the entire long isoform. The QSOX1 mAbs could be used in conjunction with an antibody against the extra residues included in QSOX1-L to look at the difference in QSOX1 concentration between QSOX1-S and QSOX1-L in the ECM and in conditioned cell culture media. The secretion of QSOX1 found here also supports the findings of Ilani et al. (2013) in which QSOX1 knockdown cells showed a disruption of the composition of the ECM and a decrease in cell attachment, and the exogenous addition of rQSOX1 refolded the ECM and restored cell attachment. In conjunction with the idea that the activity of QSOX1 that facilitates invasion occurs outside of the cell, this

data could suggest that the composition and folding of the ECM is important in cell invasion, and that the reason for increased expression of QSOX1 by cancer cells could be to configure the ECM in a way that allows the cells to invade and metastasize.

The results of these experiments support the hypothesis that mAbs against QSOX1 inhibit invasion *in vitro*. These findings are consistent with other literature which concluded that QSOX1 plays a role in facilitating invasion and that inhibition of QSOX1 by either shRNAs or small molecules reduced the invasive phenotype of tumor cells. These mAbs allow for specific inhibition of QSOX1 without needing to transduce or transfect cells. Another possible use for these mAbs is detecting QSOX1 in biological samples to investigate QSOX1 as a potential biomarker of cancer or cancer progression.

REFERENCES

Alon, Assaf, Iris Grossman, Yair Gat, Vamsi K. Kodali, Frank Dimaio, Tevie Mehlman, Gilad Haran, David Baker, Colin Thorpe, and Deborah Fass. 2012. “The Dynamic Disulphide Relay of Quiescin Sulphydryl Oxidase.” *Nature*. https://doi.org/10.1038/nature11267.

Antwi, Kwasi, Galen Hostetter, Michael J. Demeure, Benjamin A. Katchman, G. Anton Decker, Yvette Ruiz, Timothy D. Sielaff, Lawrence J. Koep, and Douglas F. Lake. 2009. “Analysis of the Plasma Peptidome from Pancreas Cancer Patients Connects a Peptide in Plasma to Overexpression of the Parent Protein in Tumors.” *Journal of Proteome Research* 8 (10): 4722–31. https://doi.org/10.1021/pr900414f.

Baek, Jin A., Phil Hyun Song, Young Hwii Ko, and Mi Jin Gu. 2018. “High Expression of QSOX1 Is Associated with Tumor Invasiveness and High Grades Groups in Prostate Cancer.” *Pathology Research and Practice*. https://doi.org/10.1016/j.prp.2018.05.019.

Clark, Leland C., Richard Wolf, Donald Granger, and Zena Taylor. 1953. “Continuous Recording of Blood Oxygen Tensions by Polarography.” *Journal of Applied Physiology* 6 (3): 189–93. https://doi.org/10.1152/jappl.1953.6.3.189.

Coppock, Donald L., Deborah Cina-Poppe, and Stephanie Gilleran. 1998. “The Quiescin Q6 Gene (QSCN6) Is a Fusion of Two Ancient Gene Families: Thioredoxin and ERV1.” *Genomics*. https://doi.org/10.1006/geno.1998.5605.

Coppock, Donald L, Cynthia Kopman, Suzanne Scandalis, and Stephanie Gilleran. 1991. “Preferential Gene Expression in Quiescent Human Lung Fibroblasts.” *Cell Growth & Differentiation* 4 (6): 483–93.

Gat, Yair, Alexandra Vardi-Kilshtain, Iris Grossman, Dan Thomas Major, and Deborah Fass. 2014. “Enzyme Structure Captures Four Cysteines Aligned for Disulfide Relay.” *Protein Science*. https://doi.org/10.1002/pro.2496.

Grossman, Iris, Assaf Alon, Tal Ilani, and Deborah Fass. 2013. “An Inhibitory Antibody Blocks the First Step in the Dithiol/Disulfide Relay Mechanism of the Enzyme QSOX1.” *Journal of Molecular Biology*. https://doi.org/10.1016/j.jmb.2013.07.011.

Hanavan, Paul D, Chad R Borges, Benjamin A Katchman, Douglas O Faigel, Thai H Ho, Chen-Ting Ma, Eduard A Sergienko, Nathalie Meurice, Joachim L Petit, and Douglas F Lake. 2015. “Ebselen Inhibits QSOX1 Enzymatic Activity and Suppresses Invasion of Pancreatic and Renal Cancer Cell Lines.” *Oncotarget* 6 (21): 18418–28. https://doi.org/10.18632/oncotarget.4099.

Heckler, Erin J., Assaf Alon, Deborah Fass, and Colin Thorpe. 2008. “Human Quiescin-Sulfhydryl Oxidase, QSOX1: Probing Internal Redox Steps by Mutagenesis.” *Biochemistry*. https://doi.org/10.1021/bi702522q.

Hoober, Karen L., Joan Burnside, Colin Thorpe, Nicole M. Glynn, and Donald L. Coppock. 2002. “Homology between Egg White Sulfhydryl Oxidase and Quiescin Q6 Defines a New Class of Flavin-Linked Sulfhydryl Oxidases.” *Journal of Biological Chemistry*. https://doi.org/10.1074/jbc.274.45.31759.

Hoober, Karen L, Bhavana Joneja, Harold B White, and Colin Thorpe. 1996. “A Sulfhydryl Oxidase from Chicken Egg White.” *Journal of Biological Chemistry* 271 (48): 30510–16.

Ilani, Tal, Assaf Alon, Iris Grossman, Ben Horowitz, Elena Kartvelishvily, Sidney R. Cohen, and Deborah Fass. 2013. “A Secreted Disulfide Catalyst Controls Extracellular Matrix Composition and Function.” *Science*. https://doi.org/10.1126/science.1238279.

Jaje, Jennifer, Holly N. Wolcott, Olajumoke Fadugba, Diane Cripps, Austin J. Yang, Ian H. Mather, and Colin Thorpe. 2007. “A Flavin-Dependent Sulfhydryl Oxidase in Bovine Milk.” *Biochemistry*. https://doi.org/10.1021/bi7016975.

Javitt, Gabriel, Iris Grossman-Haham, Assaf Alon, Efrat Resnick, Yael Mutsafi, Tal Ilani, and Deborah Fass. 2018. “Proline Mutants of Quiescin Sulfhydryl Oxidase 1 With Altered Redox Properties Undermine ECM Integrity and Cell Adhesion in Fibroblast Cultures.” *Protein Science*. https://doi.org/10.1002/pro.3537.

Katchman, B. A., K. Antwi, G. Hostetter, M. J. Demeure, A. Watanabe, G. A. Decker, L. J. Miller, D. D. Von Hoff, and D. F. Lake. 2011. “Quiescin Sulfhydryl Oxidase 1 Promotes Invasion of Pancreatic Tumor Cells Mediated by Matrix Metalloproteinases.” *Molecular Cancer Research*. https://doi.org/10.1158/1541-7786.MCR-11-0018.

Katchman, Benjamin A, I Tolgay Ocal, Heather E Cunliffe, Yu-Hui Chang, Galen Hostetter, Aprill Watanabe, Janine Lobello, and Douglas F Lake. 2013. “Expression of Quiescin Sulfhydryl Oxidase 1 Is Associated with a Highly Invasive Phenotype and Correlates with a Poor Prognosis in Luminal B Breast Cancer.” *Breast Cancer Research* 15 (2): 28. https://doi.org/doi: 10.1186/bcr3407.

Kearney, J F, A Radbruch, B Liesegang, and K Rajewsky. 1979. “A New Mouse Myeloma Cell Line That Has Lost Immunoglobulin Expression but Permits the Construction of Antibody-Secreting Hybrid Cell Lines.” *Journal of Immunology* 123 (4): 1548–50.

Knutsvik, Gøril, Karin Collett, Jarle Arnes, Lars A. Akslen, and Ingunn M. Stefansson. 2016. “QSOX1 Expression Is Associated with Aggressive Tumor Features and Reduced Survival in Breast Carcinomas.” *Modern Pathology*. https://doi.org/10.1038/modpathol.2016.148.

Mairet-Coello, Georges, Anna Tury, Annick Esnard-Feve, Dominique Fellmann, Pierre Yves Risold, and Bernadette Griffond. 2004. “FAD-Linked Sulfhydryl Oxidase QSOX: Topographic, Cellular, and Subcellular Immunolocalization in Adult Rat Central Nervous System.” *Journal of Comparative Neurology*. https://doi.org/10.1002/cne.20126.

Mitchell, Natalie M., Andrew L. Sherrard, Surendra Dasari, D. Mitchell Magee, Thomas E. Grys, and Douglas F. Lake. 2018. “Proteogenomic Re-Annotation of Coccidioides Posadasii Strain Silveira.” *Proteomics* 18 (1): 1700173. https://doi.org/10.1002/pmic.201700173.

Ning, Botao, Yongmin Tang, Hua Song, Shilong Yang, and Hongqiang Shen. 2012. “Cloning and Sequencing of the Light Chain Variable Region from NS-1 Myeloma.” *Oncology Letters*. https://doi.org/10.3892/ol.2012.601.

Pernodet, Nicolas, François Hermetet, Pascale Adami, Anne Vejux, Françoise Descotes, Christophe Borg, Marjorie Adams, et al. 2012. “High Expression of QSOX1 Reduces Tumorogenesis, and Is Associated with a Better Outcome for Breast Cancer Patients.” *Breast Cancer Research*. https://doi.org/10.1186/bcr3341.

Radom, Jean, Didier Colin, Franck Thiebault, Mai Dognin-Bergeret, Georges Mairet-Coello, Annick Esnard-Feve, Dominique Fellmann, and Michèle Jouvenot. 2006. “Identification and Expression of a New Splicing Variant of FAD-Sulfhydryl Oxidase in Adult Rat Brain.” *Biochimica et Biophysica Acta - Gene Structure and Expression*. https://doi.org/10.1016/j.bbaexp.2006.04.008.

Raje, Sonali, Nicole M. Glynn, and Colin Thorpe. 2002. “A Continuous Fluorescence Assay for Sulfhydryl Oxidase.” *Analytical Biochemistry* 307 (2): 266–72. https://doi.org/10.1016/S0003-2697(02)00050-7.

Raje, Sonali, and Colin Thorpe. 2003. “Inter-Domain Redox Communication in Flavoenzymes of the Quiescin/Sulfhydryl Oxidase Family: Role of a Thioredoxin Domain in Disulfide Bond Formation.” *Biochemistry*. https://doi.org/10.1021/bi030003z.

Rudolf, Jana, Marie A. Pringle, and Neil J. Bulleid. 2013. “Proteolytic Processing of QSOX1A Ensures Efficient Secretion of a Potent Disulfide Catalyst.” *Biochemical Journal*. https://doi.org/10.1042/BJ20130360.

Stirling, Colin J., Martin Willer, Neil J. Bulleid, Seema Chakravarthi, and Catherine E. Jessop. 2007. “Intracellular Catalysis of Disulfide Bond Formation by the Human Sulfhydryl Oxidase, QSOX1.” *Biochemical Journal*. https://doi.org/10.1042/bj20061510.

Sung, Hye-Jin, Jung-Mo Ahn, Yeon-Hee Yoon, Sang-Su Na, Young-Jin Choi, Yong-In Kim, Soo-Youn Lee, Eung-Bae Lee, Sukki Cho, and Je-Yoel Cho. 2018. “Quiescin Sulfhydryl Oxidase 1 (QSOX1) Secreted by Lung Cancer Cells Promotes Cancer Metastasis.” *International Journal of Molecular Sciences*. https://doi.org/10.3390/ijms19103213.

Vinci, Maria, Carol Box, and Suzanne A. Eccles. 2015. “Three-Dimensional (3D) Tumor Spheroid Invasion Assay.” *Journal of Visualized Experiments*, no. 9: e52686. https://doi.org/10.3791/52686.

Wang, Zhongde, Murisiku Raifu, Meredith Howard, Laurie Smith, David Hansen, Richard Goldsby, and David Ratner. 2000. “Universal PCR Amplification of Mouse Immunoglobulin Gene Variable Regions: The Design of Degenerate Primers and an Assessment of the Effect of DNA Polymerase 3’ to 5’ Exonuclease Activity.” *Journal of Immunological Methods*. Vol. 233. www.elsevier.nlrlocaterjim.

Wu, T Te, and E A Kabat. 1970. “An Analysis of the Sequences of the Variable Regions of Bence Jones Proteins and Myeloma Light Chains and Their Implications for Antibody Complementarity.” *The Journal of Experimental Medicine* 132: 211–50. https://doi.org/10.1084/jem.132.2.211.

Yu, Tiantian, Joanna R. Laird, Jennifer A. Prescher, and Colin Thorpe. 2018. “Gaussia Princeps Luciferase: A Bioluminescent Substrate for Oxidative Protein Folding.” *Protein Science* 27 (8): 1509–17. https://doi.org/10.1002/pro.3433.

Zheng, Wenyun, Wenyao Zhang, Wei Hu, Chao Zhang, and Yi Yang. 2012. “Exploring the Smallest Active Fragment of HsQSOX1b and Finding a Highly Efficient Oxidative Engine.” *PLoS ONE*. https://doi.org/10.1371/journal.pone.0040935.